JOURNAL OF APPLIED ELECTROCHEMISTRY 17 (1987) 1150–1158

Analysis of the inductance influence on the measured electrochemical impedance

B. SAVOVA-STOYNOV, Z. B. STOYNOV

Central Laboratory of Electrochemical Power Sources, Bulgarian Academy of Sciences, 1040 Sofia, Bulgaria

Received 9 February 1987; revised 31 March 1987

The high-frequency region of the impedance diagram of an electrochemical cell can be deformed by the inductance of the wiring and/or by the intrinsic inductance of the measuring cell. This effect can be noticeable even in the middle frequency range in the case of low impedance systems such as electrochemical power sources. A theoretical analysis of the errors due to inductance effects is presented here, on the basis of which the admissible limiting measuring frequency can be evaluated. Topology deformations due to the effect of inductance in the case of a single-step electrochemical reaction are studied by the simulation approach. It is shown that an inductance can not only change the actual values of the parameters (electrolytic resistance, double layer capacitance, reaction resistance), but can also substantially alter the shape of the impedance diagram, this leading to erroneous structure interpretations. The effect of the size and surface area of the electrode on its intrinsic inductance is also evaluated.

Nomenclature

A	linear dimension of the surface area confined by the circuit (cm)
C_D	double layer capacitance (F)
C_M	measured capacitance
d	diameter of the mean effective current line (mm)
f_{max}	limiting (maximum) frequency of measurement (Hz)
K_1, K_2	shape coefficients with values of $2\pi \times 10^{-9}$ and 0.7 for a circle, and 8×10^{-9} and 2 for a square (dimensionless)
L	intrinsic inductance of the electrochemical cell assumed as an additive element (H)
R_E	electrolyte resistance (Ω)
R_M	measured resistance (Ω)
R_P	reaction resistance (Ω)
r_0	specific resistance (Ω cm)
S	electrode surface area (cm^2)
T_c	time constant (s)
Z	impedance (Ω)
Z_{Im}	imaginary component of the impedance without accounting for the influence of inductance (Ω)
Z'_{Im}	imaginary component of the impedance accounting for the influence of the additive inductance (Ω)
β	shape coefficient; $\beta = 1$ for a square and $\beta = \pi^{1/2}/2$ for circle (dimensionless)
ε_L	relative complex error due to the influence of inductance (dimensionless)
ε_A^L	relative amplitude error due to inductance (%)
ε_φ^L	relative phase error due to inductance (%)
ϱ	ratio between the effective inductance time constant and the capacitive time constant (dimensionless)
ω	angular frequency (s^{-1})
ω_R	characteristic frequency at which the inductive and capacitive parts of the imaginary component of impedance are equal (s^{-1})

0021–891X/87 $03.00 + .12

1. Introduction

The development of impedance instrumentation for the high frequency range (10 kHz to 1 MHz) revealed the problem of the effect of the impedance of the electric leads and the intrinsic inductance of the electrochemical system under study on the results of the measured impedance. This problem exists even in the lower frequency ranges, when studying low-resistance systems such as electrochemical power sources and similar industrial objects with an impedance in the 1 mΩ region.

A basic method eliminating the inductance of the wiring uses a four-point circuit in the impedance measurement and has the connection of the buffer pre-amplifiers for the voltage measurement as close as possible to the object under study. If this method is properly applied the inductance and the impedance of the electric leads can be completely eliminated. However, even in this case the measured equivalent impedance includes the inductance and the intrinsic impedance of the wiring of the cell as well as the inductance pertinent to the mean effective current line electrode–electrolyte–reference electrode.

These two components determine the intrinsic inductance of the cell under study which, in principle, has distributed parameters, but as a first approximation can be considered as an element with lumped parameters. This assumption is quite reasonable at frequencies in the 10–100 kHz range, where the inductance effect is an additive quantity.

It is the aim of this paper to analyse the effect of the additive inductance from two points of view:

(i) a quantitative evaluation of the inductance errors

(ii) an evaluation of the deformations of the impedance diagrams due to inductance effects to eliminate any erroneous structure interpretations.

2. Quantitative treatment of the inductance error

In the most general case an electric system can be presented by the equivalent circuit shown in Fig. 1. The impedance of this circuit is defined by

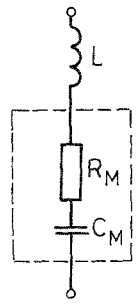

Fig. 1. Electric equivalent circuit of the measured impedance.

$$Z = R_M + j\left(\omega L - \frac{1}{\omega C_M}\right) \qquad (1)$$

In order to estimate the error due to inductance effects, the imaginary components should be compared with those of an ideal system with a zero inductance. The relative inductance error can be then expressed by

$$\varepsilon_L = \frac{Z^L_{Im} - Z_{Im}}{Z_{Im}} = -\omega^2 L C_M \qquad (2)$$

This equation indicates that the error is proportional to the square of the measuring frequency and depends on the value of L, determined from the configuration of the system under investigation, as well as on C_M, which is a specific quantity of the system. In the case of model microsystems this error is small and is noticeable only in the high frequency range, whereas in the case of large real systems, where C_M can reach several hundreds of Farads [1, 2], the error becomes significant even in the lower frequency range.

On the basis of the admissible value of the inductance error the value of f_{max} can be determined by the relation

$$f_{max} = \frac{1}{2\pi}(\varepsilon_L / L C_M)^{1/2} \qquad (3)$$

Fig. 2 presents the dependence of f_{max} on the capacitance of the system for admissible inductance errors $\varepsilon_L = 1\%$ and $\varepsilon_L = 100\%$, with inductance values close to those met in practice, i.e. $L = 1\,\mu H$ and $L = 0.1\,\mu H$. The plots reveal that systems with a capacitance of 50–100 μF can be measured correctly in the

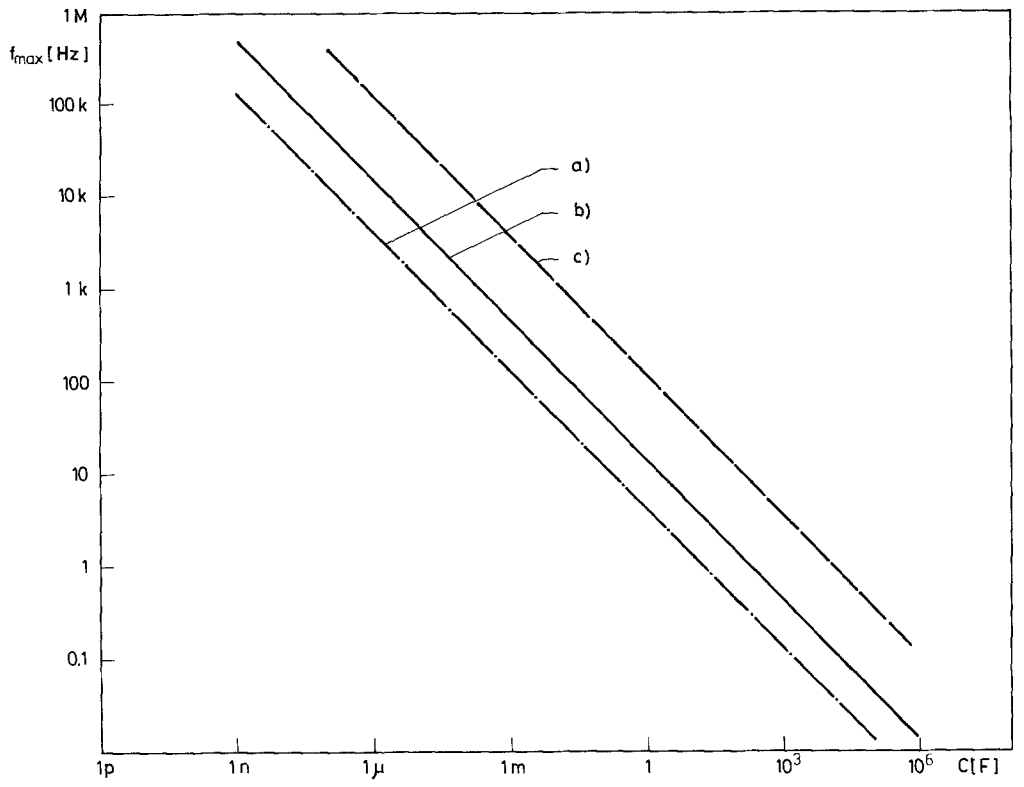

Fig. 2. Dependence of the limiting frequency on the capacitance and the error, ε_L, calculated by Equation 3. (a) $\varepsilon_L = 1\%$, $L = 1\,\mu H$; (b) $\varepsilon_L = 1\%$, $L = 0.5\,\mu H$; (c) $\varepsilon_L = 1\%$, $L = 0.1\,\mu H$; (d) $\varepsilon_L = 100\%$, $L = 1\,\mu H$.

frequency range up to 10 kHz. The relations (a) and (b) in Fig. 2 imply that a reduction in the value of L has an insignificant effect on the increase of f_{max}.

In the case of more complex impedance models of the system under study (e.g. a polarized electrode, a two-step reaction, etc.) Equations 1–3 also become more complex and the straightforward assessment of ε_L and f_{max} becomes more difficult. In addition to this, the increase in the frequency can bring about a series of changes in the ideal impedance diagram, which could lead to erroneous structural identification. In order to analyse these phenomena simulation investigations were carried out.

3. Topology investigations

The topology investigations were performed by computer simulation [3] in order to reveal the structural deformations which could arise by the influence of inductance on the plotted impedance diagram. The simulations were carried out in the 1 to 10^6 Hz range by variation of the factor ϱ, which is a function of the parameters included in the model, namely

$$\varrho = L/R_p^2 C_D \tag{4}$$

The factor ϱ represents the ratio between the inductance and capacitance time constants ($\varrho = T_L^*/T_C$) where $T_L^* = L/R_p$ is the effective time constant.

The observed topological changes in the impedance diagram have been shown in a three-dimensional presentation ($-I_m$, R_e, $\log \omega$), which considerably facilitates the assessment of the structural deformation.

3.1. *Ideal non-polarized electrode (INPE)*

The electric equivalent circuit of this simplest electrochemical system is shown in Fig. 3a. The impedance is expressed by

$$Z = R + j\omega L \tag{5}$$

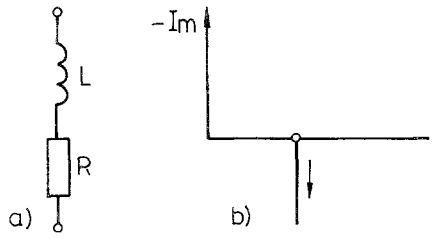

Fig. 3. (a) Electric equivalent circuit of an ideal non-polarized electrode; (b) the impedance diagram.

The impedance diagram of INPE presented in Fig. 3b reveals that the behaviour of the imaginary component is purely inductive. The error due to induction (amplitude and phase) is given by

$$\varepsilon_A^L = [(\omega^2 L^2 + R^2)^{1/2}/R] - 1$$
$$\varepsilon_\varphi^L \approx \omega L/R \qquad (6)$$

while the limiting measuring frequency as a function of ε_A^L and ε_φ^L is determined by

$$f_{max} = \frac{R}{2\pi L}(\varepsilon_A^2 + 2\varepsilon_A)^{1/2}$$
$$f_{max} = (R/2L)\varepsilon_\varphi^L \qquad (7)$$

Fig. 4 illustrates the dependence of the limiting frequency on the resistance of the system at $L = 1\,\mu H$. The limiting frequency for systems with resistances in the mΩ range and an admissible error of 1% lies between 100 and 1000 Hz, while for an error of 0.1% or 1° it drops to the 10–100 Hz range.

This is the case in the investigation of exceptionally low ohmic electrochemical power sources, e.g. the sodium–sulphur cell, where the inductance effect becomes predominant even before the appearance of the basic high-frequency components of the impedance [4].

3.2. *Ideal polarized electrode (IPE)*

The total impedance of this system (Fig. 5) is

$$Z = R_E + j\left(\omega L - \frac{1}{\omega C_D}\right) \qquad (8)$$

In this case the capacitance component of the impedance decays with increase of frequency and tends to zero. Above a definite frequency it can even change sign and begin to grow, i.e. it becomes an inductive component (Fig. 6a, b).

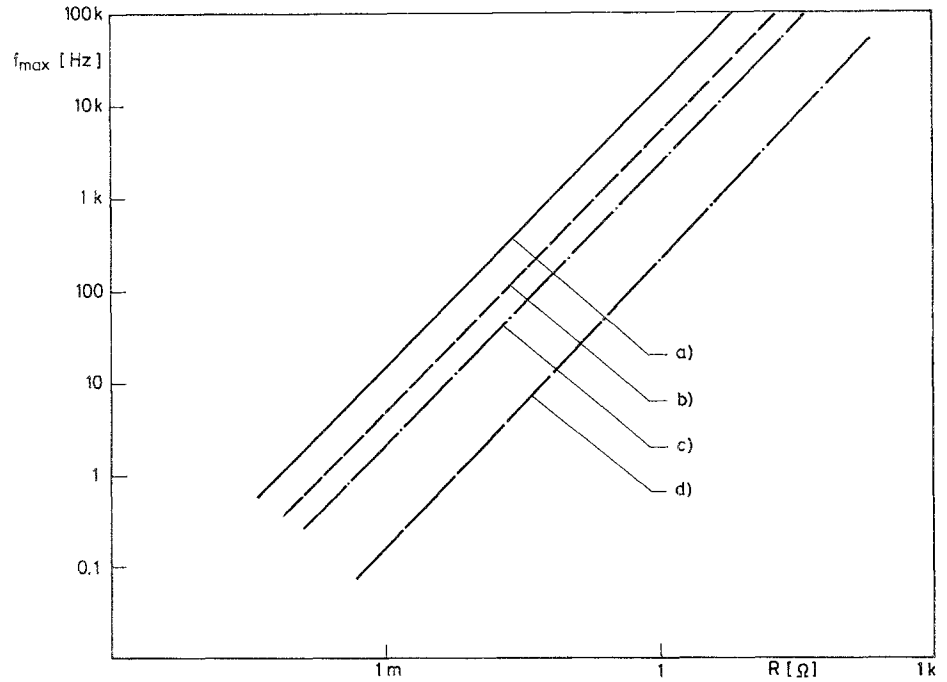

Fig. 4. Dependence of the limiting frequency on the resistance of the system at $L = 1\,\mu H$: (a) $\varepsilon_A^L = 1\%$; (b) $\varepsilon_A^L = 0.1\%$; (c) $\varepsilon_\varphi^L = 1°$; (d) $\varepsilon_\varphi^L = 0.1°$.

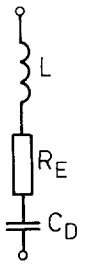

Fig. 5. Electric equivalent circuit of an ideal polarized electrode.

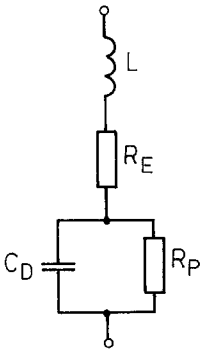

Fig. 7. Electric equivalent circuit of one-step reaction.

3.3. *One-step reaction (Faradaic reaction)*

Depending on the ratio of the parameters L, C_D, and R_P (Fig. 7) the shape of the impedance diagram can change, whereby one of the following typical cases may be observed (Fig. 8a–c).

The general expression of the impedance is

$$Z = R_E + j\omega L + \left(\frac{1}{j\omega C_D + 1/R_P}\right) \quad (9)$$

At low L values (Fig. 8a) the impedance diagram is represented approximately by a regular semicircle, close to that for $L = 0$, and by a high-frequency part with inductive origin. In this case one can observe points which are concentrated in the vicinity of the frequency, ω_R, which become more apparent in the $I_m/\log\omega$ plane in the form of an inflection. The deviations of the I_m component from the regular semicircle are insignificant and the error is given by Equation 2. In this case the influence of the inductance is weak, only parametric, the error is small, and the semicircle can be treated as inductance-free. The presence of concentrated points is an indication that the system under study pertains to this case, but numerical values of the parameters can be obtained only after an appropriate identification.

As the relative value of L is increased, the shape and size of the semicircle are retained but the concentrated points disappear (Fig. 8b). In the $I_m/\log\omega$ presentation the inflection also disappears and the curve intercepts the $\log\omega$ axis very steeply. This leads to the conclusion that a numerical identification from the $(-I_m)$ region only is not reasonable in the case of a model which does not take into account L, and the three-dimensional presentation can be only used to facilitate a qualitative evaluation.

As L is further increased the semicircle maintains its shape, changing only in size, but its intercept on the real axis deviates from the value of R_E (Fig. 8c). The error in the calculation of R_E due to the effect of L is given by

$$\varepsilon^L_{RE} = \varrho(R_P/R_E) \quad (10)$$

while that in the evaluation of R_P is

$$\varepsilon^L_{RP} = -\varrho \quad (11)$$

where

$$\varrho = L/R_P^2 C_D \quad (12)$$

On the basis of the factor ϱ the equation for the characteristic frequency can be written as

$$\omega_R = \frac{1}{T}\left(\frac{1}{\varrho} - 1\right)^{1/2} \quad (13)$$

These estimates (Equations 10–13) are valid for values of ϱ in the 0–1 range. At values of ϱ approaching 1 the diagram is strongly deformed

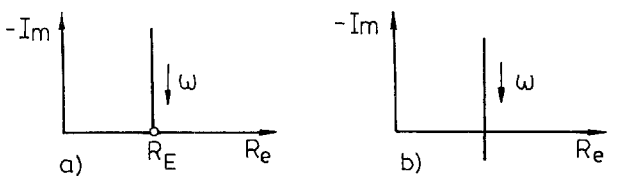

Fig. 6. Impedance diagram of the ideal polarized electrode at (a) $L = 0$, (b) $L \neq 0$.

(Fig. 8d), while at $\varrho = 1$ ($\omega_R = 0$) its shape is so degenerated that only the $+I_m$ component remains (Fig. 8*e*).

Figs 8f and 8g present the cases when $\varrho > 1$. Typical deformations appear which initially are parallel to the I_m axis and have a typical S-shape. This shape is a direct evidence for the presence of a high-frequency process, hidden by the effect of inductance.

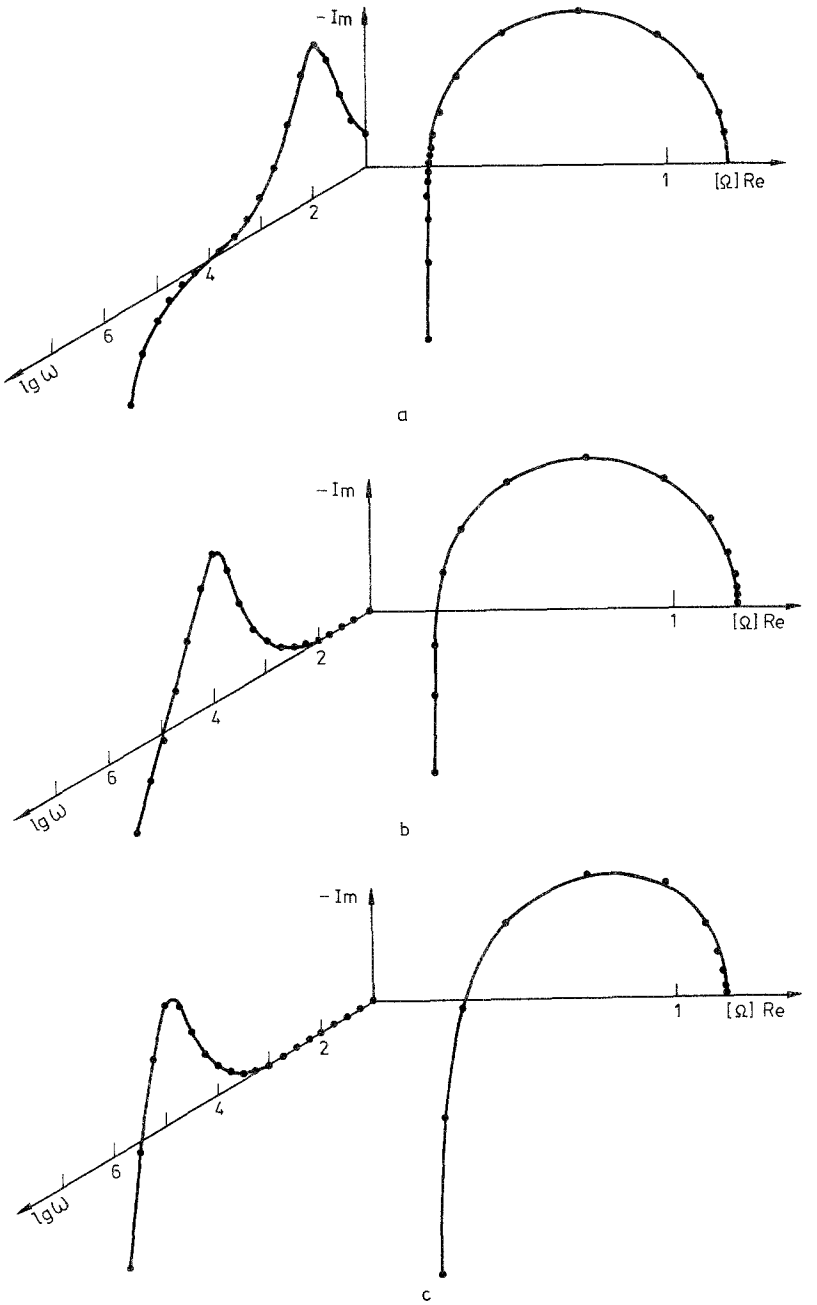

Fig. 8. Simulated impedance diagrams of one-step reaction model influenced by inductance; $\omega = 1$–10^6; $L = 1\,\mu H$; $R_E = 0.2\,\Omega$; $R_P = 1\,\Omega$. Variation of the factor $\varrho = f(L, R_P, C_D)$: (a) $\varrho = 0.0001$; (b) $S = 0.01$; (c) $\varrho = 0.1$; (d) $\varrho = 0.5$; (e) $\varrho = 1$; (f) $\varrho = 2$; (g) $\varrho = 5$.

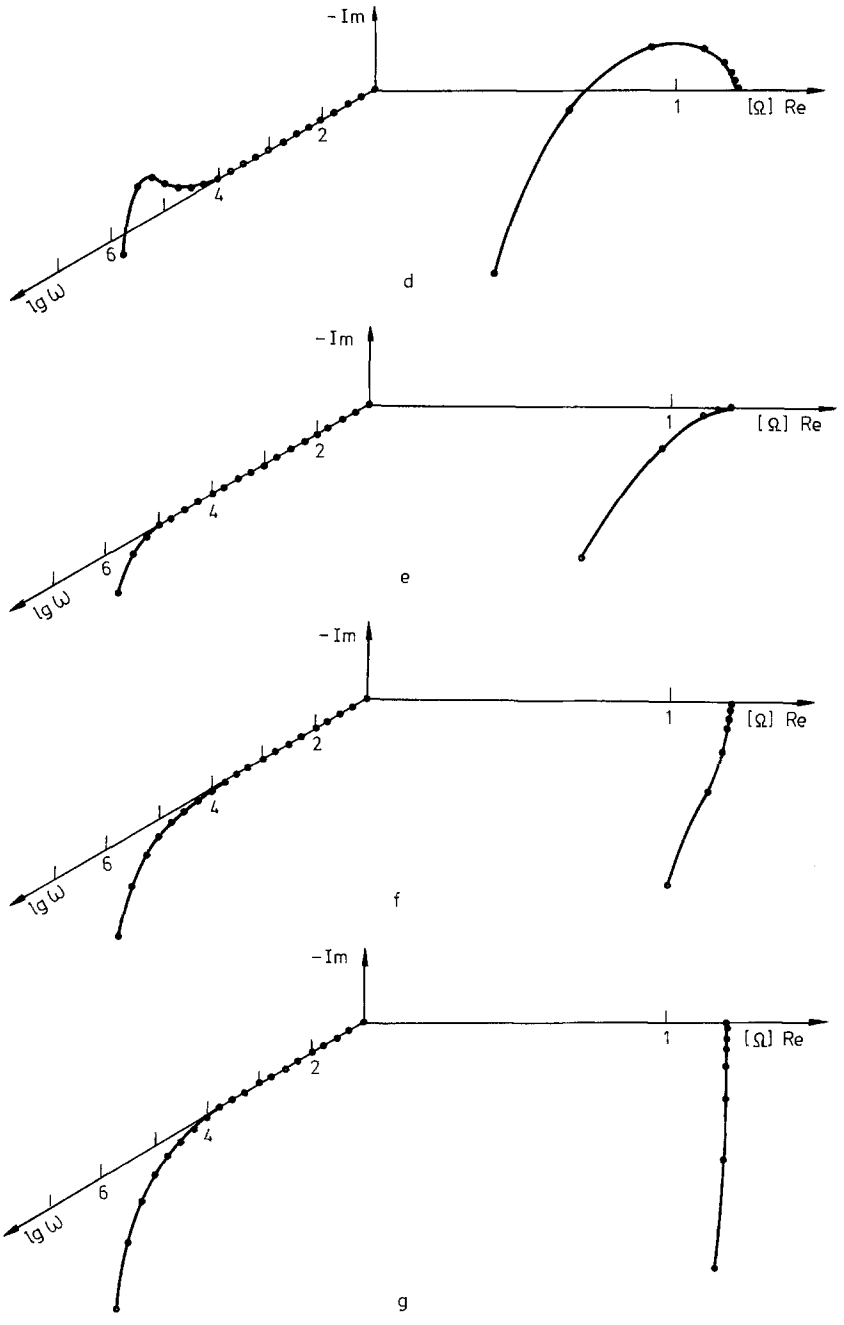

Fig. 8. Continued.

4. Dependence of the inductance on the configuration and surface area of the measured electrode

The effect of the cell inductance on the measured impedance can be reduced by optimization of the shape and size of the measured electrode. From this point of view the cell can be considered as a one-loop circuit, comprising the electrode under study, the electrolyte, the reference electrode and at least part of the leads of both electrodes, whereby the circuit coincides with the

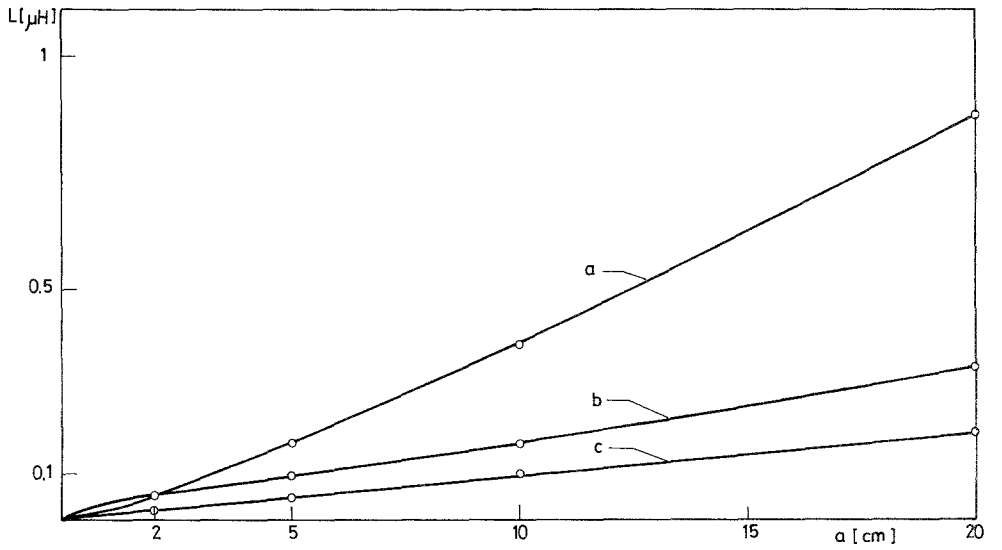

Fig. 9. Dependence of the inductance on the linear dimension of a single-loop circuit for: (a) square shape with a linear dimension a, wire diameter 1 mm; (b) rectangular shape with a linear dimension $2a$, wire diameter 1 mm; (c) same shape and dimension, wire diameter 5 mm.

mean current line determined by the cell configuration. It is well known from theoretical electrotechnics that the inductance of a single-loop circuit is determined by its dimensions and geometry as well as by the diameter of the wire [6].

Fig. 9 illustrates the dependence of this inductance on the linear dimensions of the circuit as a function of the shape and diameter of the wire. From the relationships in Fig. 9a, b it is evident that at one and the same diameter the inductance grows with the area encircled by the wire. The wire diameter has also a considerable effect on the inductance, which diminishes as the diameter is increased (Fig. 9c).

In order to evaluate the effect of the surface area of the electrode under study on the inductance error, the following expression for the resistance is introduced in Equation 11:

$$R = r_0/S \tag{14}$$

which yields an expression for the error as a function of the electrode surface area

$$\varepsilon_R^L = LS/T_c r_0 \tag{15}$$

Expressions for the calculation of the inductance of a single-loop circuit as a function of the shape and dimensions of the circuit are given by theoretical electrotechnics [6]. After introducing some simplifications the following equation can be derived

$$L = K_1 A \ln (2K_2 A/d) \tag{16}$$

By the combination of Equations 15 and 16 a general equation for the inductance error as a function of the electrode surface area is obtained:

$$\varepsilon_L = \frac{\beta K_1}{T r_0}\left[S^{1.5}(0.5 \ln S + \ln \frac{2K_2}{d} + \log \beta)\right] \tag{17}$$

where $T = R_P C_D$ and r_0 are electrochemical parameters, and K_1, K_2, S, d, and β are geometric parameters.

After simplification it can be concluded that the error is approximately proportional to the square of the surface area of the electrode investigated.

5. Discussion

The effect of the intrinsic impedance of the cell under investigation on the measured electrochemical impedance has been studied from two points of view: a qualitative evaluation of the parametric errors and an analysis of the structural alterations in the impedance diagram.

Analytical expressions have been derived for

the estimation of the inductance error and for f_{max} at a preselected error value. It is established that in the case of low resistance systems f_{max} shifts to the range of the middle and low frequencies. Hence, one should be cautious, especially when measuring high-capacity electrochemical power sources, where significant inductance errors can arise at frequencies as low as 10–1000 Hz.

The analysis performed in this paper reveals that a considerable increase of the useful measuring frequency range can be achieved by the miniaturization of the experimental cell (e.g. by reducing the mean current line and, especially, reducing the electrode surface area). This leads to the use of model electrodes with which it is possible to study fast processes. An important role is assigned here to the configuration of the experimental cell which, in the optimum case, should be coaxial. The influence of the external wiring can be also significant. This problem is not considered in this paper, but has been elucidated in detail by Göhr *et al.* [7]

The considerations presented here lead to some important conclusions as regards experimental methods and instrumentation. The measuring frequency range should also include the region where inductance is relevant. In this way one can obtain data allowing for the application of appropriate algorithms for the identification and correction of its influence. As a result of this procedure f_{max} can be increased considerably.

In the study of fast processes which are completely concealed by the effect of inductance (Fig. 8e–g), it is necessary to develop special instrumentation and methods permitting investigations under predominant inductance conditions.

References

[1] M. Keddam, Z. Stoynov and H. Takenoutti, *J. Appl. Electrochem.* **7** (1977) 539.

[2] Z. Stoynov, 28th ISE Meeting, Extended Abstracts, Varna (1977) p. 148.

[3] Z. Stoynov and B. Savova-Stoynov, *J. Electroanal. Chem.* **209** (1986) 11.

[4] G. Staikov, P. D. Yankulov, B. S. Savova-Stoynov and Z. B. Stoynov, *J. Appl. Electrochem.* **15** (1985) 895.

[5] Z. Stoynov and B. Savova-Stoynov, *J. Electroanal. Chem.* **170** (1984) 63.

[6] 'Elektrotekhnicheskii Spravochnik', Vol. 1, Gosenergoizdat, Moscow (1955).

[7] H. Göhr, M. Mirink and C. A. Schiller, *J. Electroanal. Chem.* **180** (1984) 273.